sciendo

Transport and Telecommunication, 2023, volume 24, no. 3, 320–337
Transport and Telecommunication Institute, Lomonosova 1, Riga, LV-1019, Latvia
DOI 10.2478/ttj-2023-0026

OPTIMIZATION TURBINE BLADE COOLING BY APPLYING JET IMPINGEMENT COOLING CHANNELS

Adham Ahmed Awad Elsayed Elmenshawy[1], Iyad Alomar[2], Ali Arshad[1]

[1]Riga Technical University
Riga, Latvia
Adham-Ahmed-Awad-Elsayed.Elmenshawy@rtu.lv
Ali.Arshad@rtu.lv
[2]Transport and Telecommunication Institute
1 Lomonosov Str., Riga, LV-1019, Latvia
alomar.i@tsi.lv

The aim of this paper is to optimize turbine blade cooling channels by applying jet impingement Method. The selection of experiment data for NASA 3CX turbine blade, and 3D model using solidworks software and create computational fluid dynamics (CFD) simulations used to model the coolant flow and temperature distribution in the vane, while experimental testing can validate the CFD results and provide additional insights into the cooling system's performance., ANSYS FLUENT code was used as a CFD solver, and ANSYS ICEM-CFD was used for mesh generation. MATLAB code is used for calculation using experiment data and this was helpful for simulations. Heat transfer conjugation analysis bases SST shear stress analyses K-ω turbulent model. The results conclude that providing additional information about the cooling channels and how they differ in the studies being compared. The results demonstrate that the cooling channels' hydraulic diameter decreases by a significant percentage (up to 49.70%-69.55%) as they are drawn to the trailing edge of the blade. This can have a significant impact on the heat transfer coefficients and the performance of the cooling system. The pressure side of the turbine blade is observed to follow the Hylton Model, while the current study predicts a large over-anticipated heat transfer coefficient around the Turbine blade head and on the bulk of the suction side. In terms of average heat transfer coefficient, the two models differ by 23.36%. The authors found that the cooling effectiveness for the Optimized jet impingement model is 0.4892 for whole blade and compared it with the cooling effectiveness for the optimized jet impingement model, which is 0.6936, The results of the comparison between the base model and the optimized jet impingement model suggest that the optimized model has a significantly higher cooling effectiveness. The increase in cooling effectiveness of 29.46% for the whole blade and 28.823% for the trailing edge indicates that the optimized jet impingement design provides improved cooling performance. These results highlight the importance of considering optimized cooling designs for turbine blades to maintain efficient and safe operation.

Keywords: Conjugate heat transfer, thermal performance, turbine blade cooling channels

1. Introduction

A turbine blade failure due to cooling problems can have serious consequences for the performance and reliability of a gas turbine engine (Nozhnitsky, 2018). By raising the temperature of the gas entering the turbine, the amount of energy that can be extracted from the combustion process increases, resulting in improved efficiency. However, the higher temperatures also put additional stress on the turbine blades, which can affect their strength and durability (Yamane *et al.*, 2012). This requires the use of materials with improved heat resistance, as well as advanced cooling techniques to maintain safe operating conditions for the blades. The industry is constantly seeking ways to improve the balance between increasing temperature and ensuring safe operation (Ackert, 2011; Zaretsky *et al.*, 2013). Cooling problems can arise from a variety of issues, such as clogged cooling passages, insufficient flow rate, or inadequate coolant temperature, which can result in overheating and damage to the turbine blades. If a blade fails, it can cause damage to other engine components, disrupt the airflow, and lead to unbalanced rotations, leading to significant engine vibration and possible complete engine failure (Elmenshawy and Alomar, 2022). Proper cooling design and maintenance of the cooling system is essential to avoid such problems and ensure safe and efficient operation of the gas turbine engine (Coletti *et al.*, 2012). The use of advanced cooling configurations, optimization methods, and Conjugate heat transfer (CHT) analyses has been critical in addressing the challenges posed by increasing turbine inlet temperatures. These cooling configurations aim to provide an

optimal balance between providing sufficient cooling to the blades while minimizing any potential losses in efficiency. The optimization methods help in finding the most effective cooling strategies by using numerical simulations and models (Nirmalan and Hylton, 1989). CHT analyses help in better understanding the heat transfer processes within the blades, allowing for improvements in cooling design and performance. By combining these techniques, engineers and researchers in the gas turbine industry can develop cooling solutions that effectively manage the high temperatures while ensuring safe and reliable operation of the engine. In this specific study, ANSYS FLUENT code was used as a CFD solver, and ANSYS ICEM-CFD was used for mesh generation. ANSYS ICEM-CFD used to generate high-quality meshes that are suitable for use in CFD simulations. Together, these tools can be used to perform detailed and accurate CFD simulations of the cooling configurations in a gas turbine blade. This study is providing additional information about the cooling channels and how they differ in the studies being compared. The results presents that the cooling channels hydraulic diameter decreased by a significant percentage (up to 49.70%-69.55%), as they get closer to the vane's trailing edge. This can have a significant impact on the heat transfer coefficients and the performance of the cooling system. The results present the cooling effectiveness for Hylton Model was 0.4892 for whole blade and we compare it with the cooling effectiveness for the optimized jet impingement model, which is 0.6936, The results of the comparison between the base model and the optimized jet impingement model suggest that the optimized model has a significantly higher cooling effectiveness. The increase in cooling effectiveness of 29.46% for the whole blade and 28.823% for the trailing edge indicates that the optimized jet impingement design provides improved cooling performance. These results highlight the importance of considering optimized cooling designs for turbine blades to maintain efficient and safe operation.

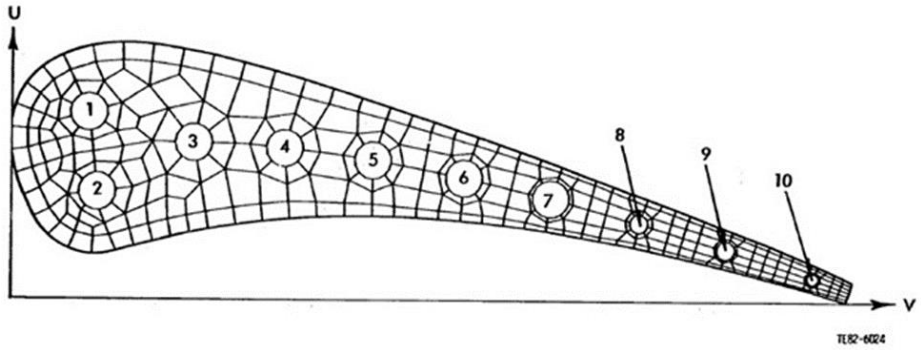
2. Methodology

The importance of considering optimized cooling designs for turbine blades to maintain efficient and safe operation Computational Fluid Dynamics (CFD) is a powerful tool that can be used to design cooling configurations in gas turbine blades. CFD simulations can provide detailed predictions about the flow and heat transfer trends within the turbine blade, which can be used to optimize the cooling design and improve the thermal performance of the blade and here the methods used in this research:

- Collection of experiment data for NASA C3X using Hylton Model (Hylton and York, 1985; Nirmalan and Hylton, 1989) data from experimental tests of the gas turbine blade cooling configuration to use as a basis for the CFD simulation.
- Setting up the basic geometry and dimensions of the simulation domain, which includes the gas turbine blade and the surrounding fluid domain.
- Selecting the appropriate model to use for simulating heat transfer between the gas turbine blade and the surrounding fluid, which is conjugate heat transfer (CHT) model.
- Selecting the appropriate model to use for simulating turbulence within the fluid domain, which is the SST k-omega.
- Modelling the design by creating a detailed 3D CAD model of the gas turbine blade and the cooling configuration using SolidWorks.
- Creation of MATLAB algorithm and developing a custom MATLAB code to perform the necessary numerical calculations for the CFD simulation.
- Mesh generation using ANSYS ICEM-CFD to generate a high-quality mesh that accurately represents the geometry of the gas turbine blade and the surrounding fluid domain.
- CFD simulation using ANSYS FLUENT as the CFD solver to perform the actual simulation, using the selected heat transfer and turbulence models, as well as the custom MATLAB code for numerical calculations.

2.1. Initial Base model Configuration

NASA C3x Airfoil Vane coordinates are given in Figure 1 which presents cascade coordinate systems which is used to define the airfoil shape, the van was cooled by 10 radial cooling channels. Each hole configuration for C3X vane is shown in Figure 1. Solid works used to produce an outline the spline's feature points were obtained by using the individual coordinates found in Hylton's experiment.



Hole No.	U--cm (in.)	V--cm (in.)	Diameter--cm (in.)	Cr
1	2.377 (0.936)	1.311 (0.516)	0.630 (0.248)	1.118
2	1.057 (0.416)	1.534 (0.604)	0.630 (0.248)	1.118
3	1.981 (0.780)	3.119 (1.228)	0.630 (0.248)	1.118
4	1.981 (0.780)	4.674 (1.840)	0.630 (0.248)	1.118
5	1.869 (0.736)	6.182 (2.434)	0.630 (0.248)	1.118
6	1.666 (0.656)	7.747 (3.050)	0.630 (0.248)	1.118
7	1.412 (0.556)	9.235 (3.636)	0.630 (0.248)	1.118
8	1.087 (0.428)	10.759 (4.236)	0.310 (0.122)	1.056
9	0.737 (0.290)	12.253 (4.824)	0.310 (0.122)	1.056
10	0.345 (0.136)	13.757 (5.416)	0.198 (0.078)	1.025

Figure 1. Finite element grip structure for Nasa c3x with cooling channel's locations

The 3D model was utilized in Ansys 19.2 fluent for running CHT (Conjugate Heat Transfer) analysis on both the original and optimized designs for the cooling channels. Figure 2 presents the original 3D design of the C3X turbine blade. Hylton incorporated the Cr(correction coefficient) constant into a modified Nusselt Number expression that considered the effects of the thermal entrance region (Hylton and York, 1985).

Hylton stated that the Cr constant is a function of Pr (Prandtl number), ReD (Reynolds number based on diameter), and x/D (distance from the leading edge normalized by diameter). (Hylton and York, 1985) . The Cr(correction coefficient) constant from 1.03 to 1.12 was used to Nu (Nusselt number) calculation, and HTC (heat transfer coefficient) for 10 cooling channels(Nirmalan and Hylton, 1989). The Nu and heat transfer coefficient were then compared with Hylton's, Wang's, and the baseline configuration data from the current study (Wang *et al.*, 2015).

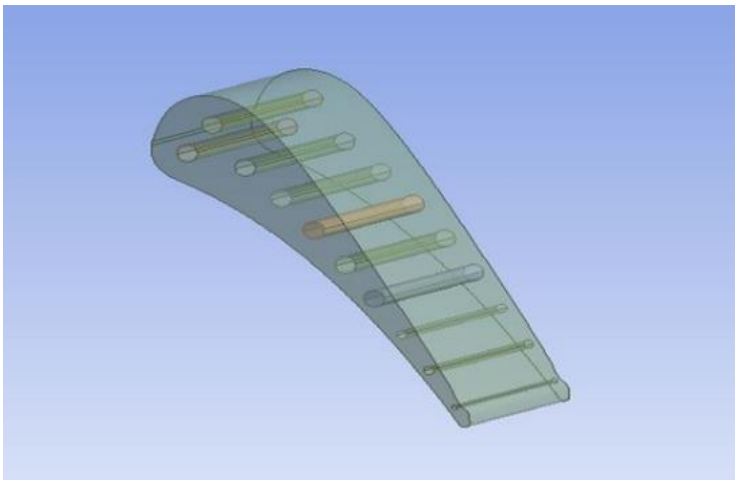


Figure 2. Base model turbine blade cooling

2.2. Mathematical Model

The governing equations used for this study are the continuity equation Eq (1), the time averaged Navier-Stokes (NAS) and the energy equations for turbulent model. In the present mathematical model, the incompressible and Momentum equation Eq (1-6) was used.

Continuity equation:

$$\frac{\partial u}{\partial x}+\frac{\partial \varphi}{\partial y}+\frac{\partial u}{\partial z}\ =0. \tag{1}$$

Momentum equation:

$$\rho_{hf}\left(u\frac{\partial u}{\partial x}+v\frac{\partial u}{\partial y}+\omega\frac{\partial u}{\partial z}\right)=-\frac{\partial p}{\partial x}+\mu_{nf}\left(\frac{\partial_u^2}{\partial x^2}+\frac{\partial_u^2}{\partial y^2}+\frac{\partial^2 u}{\partial z^2}\right). \tag{2}$$

$$\rho_{hf}\left(u\frac{\partial v}{\partial x}+v\frac{\partial v}{\partial y}+\omega\frac{\partial u}{\partial z}\right)=-\frac{\partial p}{\partial y}+\mu_{nf}\left(\frac{\partial_v^2}{\partial x^2}+\frac{\partial_v^2}{\partial y^2}+\frac{\partial^2 v}{\partial z^2}\right). \tag{3}$$

$$\rho_{hf}\left(u\frac{\partial w}{\partial x}+v\frac{\partial w}{\partial y}+\omega\frac{\partial w}{\partial z}\right)=-\frac{\partial p}{\partial z}+\mu_{nf}\left(\frac{\partial_w^2}{\partial x^2}+\frac{\partial_w^2}{\partial y^2}+\frac{\partial^2 w}{\partial z^2}\right). \tag{4}$$

Where u, v, and w are the velocity components in the x, y, and z directions. μ is Dynamic Viscosity, P is the pressure and ρ is the density. The energy derivation relation equations has been used.

Energy equation:

$$\frac{\partial}{\partial x_i}\left(\rho u_i\ C_pT-k\frac{\partial T}{\partial x_j}\right)=u_i\frac{\partial p}{\partial x_i}\mu\left(\frac{\partial u_i}{\partial x_j}+\frac{\partial u_j}{\partial x\ddot{\imath}}\right)-\frac{2}{3}\ \mu\frac{\partial u_k}{\partial x_k}\delta_{ij}, \tag{5}$$

where, ρ = the density of the fluid ; u_i represents the velocity component in the i-th direction; C_p is the specific heat capacity at constant pressure; T is the temperature; k is the thermal conductivity of the fluid; ∂_T/∂_{xj} represents the partial derivative of temperature with respect to the j-th coordinate; ∂_p/∂_{xi} represents the partial derivative of pressure with respect to the i-th coordinate; μ is the dynamic viscosity of the fluid; $(\partial_{ui}/\partial_{xj})$ represents the partial derivative of the velocity component in the i-th direction with respect to the j-th coordinate; $(\partial_{uj}/\partial$xi) represents the partial derivative of the velocity component in the j-th direction with respect to the i-th coordinate; δ_{ij} is the Kronecker delta, which is 1 when i = j and 0 otherwise.

Turbulent flow model: The Wang-RSM model is a type of Reynolds Stress Model (RSM) and differs from other commonly used models for turbulence, such as the Shear Stress Transport (SST) k-ω model, the Standard k-ω model, the k-kl-ω model, and the k-ε model (Wang *et al.*, 2015). The SST k-ω model is a turbulence model that uses two equations and combines the benefits of the k-ω and k-ε models. Specifically, it utilizes the k-ω model close to walls and the k-ε model in the outer region of the boundary layer. The SST k-ω model is popular because of its ability to accurately predict a wide range of flow types and geometries while being robust. In this study the authors used SST k- ω Model which helps to intended for turbulent flows with large-scale anisotropy, especially cooling channels. Equations (6-7) present SST k-ω Model.

$$\rho\left(\frac{\partial k}{\partial t}+\ u\ \cdot\ \nabla k\right)=\ \nabla\ \cdot\ \left[\left(\mu t\ +\frac{\mu t}{\sigma k}\right)\nabla k\right]+\ Pk-\ \beta*\rho k\omega\ +\ S, \tag{6}$$

where k - turbulence kinetic energy; μt - turbulent viscosity; Pk - turbulence production term; β – coefficient of turbulent Prandtl number; ω - specific dissipation rate; σk - turbulent Prandtl number for k; S - source term due to buoyancy and external forces

$$\rho\left(\frac{\partial \omega}{\partial t}+\ u\ \cdot\ \nabla\omega\right)=\ \nabla\ \cdot\ \left[\left(\mu t\ +\frac{\mu t}{\sigma\omega}\right)\nabla\omega\right]+\ \beta\rho\left(\frac{\omega k}{k}\right)*\ \left(\frac{Pk}{\omega}\right)-\ \beta\rho\omega^2+\ St, \tag{7}$$

where ω - specific dissipation rate of k; μt - turbulent viscosity; σω - turbulent Prandtl number for ω; St - source term due to buoyancy and external forces.

To calculate turbulent viscosity for this model the authors used Eq (8)

$$\mu t\ =\frac{\rho C\mu k^2}{\omega}, \tag{8}$$

where Cμ - constant, typically set to 0.09; k - turbulence kinetic energy; ω - specific dissipation rate of k; ρ - density.

For pressure drop calculation the authors used eq (9) which is based on the Darcy-Weisbach equation (Brown, 2002). This equation assumes that the flow is fully developed, turbulent, and incompressible, and that there are no significant changes in elevation or velocity along the length of the channel or pipe.

$$\Delta P = f\frac{L}{D}\frac{\rho U^2}{2g}, \quad (9)$$

where ΔP - pressure drop, f - friction factor, L - length of the channel or pipe, D - diameter of the channel, ρ - density, U - mean velocity of the fluid, and g - gravitational acceleration.

2.3. Heat transfer conjugation

Heat transfer conjugation includes three different physical heat transfers: external area sides, flow, heat transfer, internal cooling passages and ducts inside the blade structure. In the conjugate method, combined outer and inner flow and heat transfer with the blade line. The temperature distribution of the blade is determined by analysing these three sections. result external flow and heat transfer simulation boundary conditions for the calculation of metal wires. Internal boundary conditions for line calculations defined by simulation of internal heat and fluid flow coolant channel. As mentioned in the previous section, 3D simulation of heat transfer by internal cooling blade complex cooling passages are time consuming.

Wang experiment, the centre vane of the C3X transonic turbine was cooled by air flowing from the hub to the deck through ten circular flow channels. The blade material was specified as ASTM Type 310 stainless steel. The experiment was modelled by Wang to ASTM 310 stainless steel with a specific heat (Cp) =502 J.K/kg, Density (ρ) =8030 kg/m3, and thermal conductivity varying by temperature displayed equation (10) below (Wang, Li and Zhu, 2014; Wang *et al.*, 2015)

$$Kss = 0.0155T + 9.9105 \text{ (W.K/m)}. \quad (10)$$

Sutherland's formula was used to describe the viscosity and thermal conductivity in the simulation. The specific heat capacity, viscosity, and thermal conductivity are all temperature dependent. The viscosity is represented by μ and the thermal conductivity by Kfg. This means that these properties change with temperature, and their values can be calculated based on temperature-dependent formulas (see Equations 11 and 12) (Organ, 2007):

$$\mu(T) = \mu_0 \left(\frac{T}{T_0}\right)^{\frac{3}{2}} \times \frac{T_0+s}{T+s}. \quad (11)$$

$$k_{fg}(T) = \lambda_0 \left(\frac{T}{T_0}\right)^{3/2} * \frac{T_0+S}{T+S}. \quad (12)$$

The constants defined as λ_0= 0.0261 W/ (m·K), μ0=1.7894 x 10-5, Pa·s, T0 = 273.11 K, and S = 110.56. The Specific heat capacity of the solid, Csf was represented by an approximate polynomial fitting (Wang *et al.*, 2015):

$$C_sf = a_0 + a_1T^2 + a_2T^2 + a_3T^2 + a_4T^2. \quad (13)$$

The Reynolds Number, and hydraulic diameter were calculated for each cooling hole based on the fluid mass flow rate ṁ, hydraulic diameter for cooling channel DC, viscosity of the coolant μ, and the density of the coolant ρ. The calculation was carried out to match the outlet pressure, which required the inlet Reynolds number (ReD) to match the data from NASA C3X. Reynolds number is a crucial factor in determining the flow behaviour within each cooling channel. If the flow is turbulent, it is more likely to result in maximum heat transfer, but this type of flow also creates transitional flow regimes, When the flow is in a transitional regime, it can create challenges for simulations to accurately predict the flow behaviour and heat transfer within the cooling system. The coolant inlet ReD number was calculated based on the (DC) hydraulic diameter of each channel using the equation displayed below. Equation (14) is used to determine the characteristics of each of the individual cooling passages:

$$R_{eD} = \frac{\frac{\dot{m}}{A}Dc}{\mu}. \quad (14)$$

The 3D dimensional calculation domain for the conjugation of heat transfer around the NASA C3X plate was modelled only once to validate the heat transfer coefficient distribution around the plate and to perform calculations. The 3D domain for the conjugate heat transfer simulation is depicted in Figure 3.

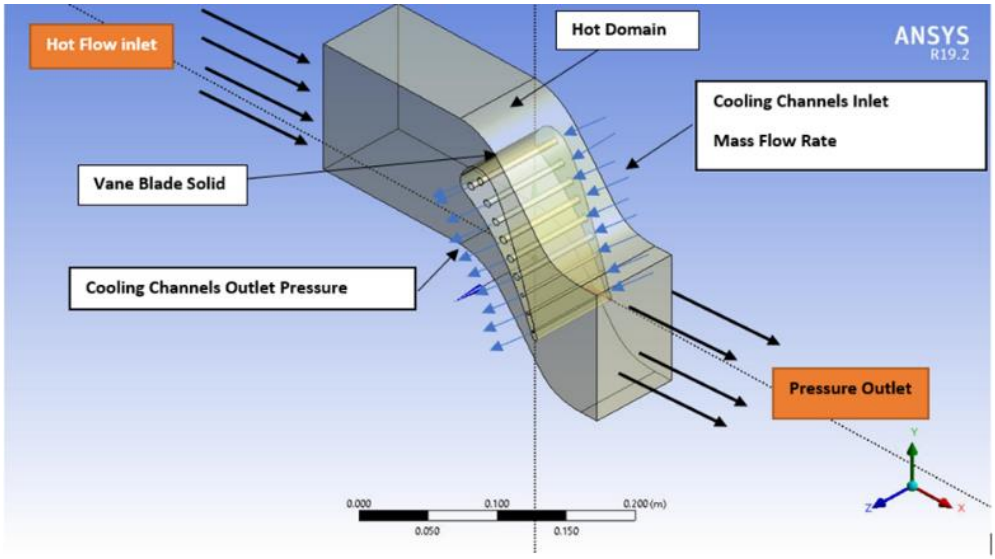


Figure 3. The 3D domain for the conjugate heat transfer simulation

The use of Computational Fluid Dynamics (CFD) and various meshing techniques, such as prism layer for meshing, polyhedral mesh, and cylinder mesh generalized, were utilized in the current study to design, and analyse the cooling configurations in a gas turbine blade. The goal was to achieve the greatest cooling efficacy while minimizing the impact on the thermodynamic system, as measured by the heat transfer coefficient (HTC). The study also compared the results to data from previous studies by Hylton and Wang. The Nusselt Number equation was used to determine the HTC of each cooling channel:

$$N_{uD} = Cr\left(0.022 p_r^{0.5} R_e^{0,8}\right). \tag{15}$$

The average heat transfer coefficient (HTC) is an important parameter in the design of cooling systems for gas turbine blades. It is used to quantify the amount of heat transferred from the metal to the coolant, and is typically expressed in units of W/m^2-K. The HTC is determined by several factors, including the fluid properties, flow conditions, and geometrical parameters of the cooling system. The Nusselt number (Nu) equation, which relates the HTC to the fluid properties and flow conditions, is commonly used to calculate the HTC. The correction coefficient (Cr), Prandtl number (Pr), and Reynolds number (ReD) are key parameters in the Nu equation and are used to account for the effects of fluid properties, flow conditions, and geometrical parameters on the HTC. The HTC values calculated using the Nu equation can then be used to compare the cooling performance of different cooling configurations and to optimize the design of the cooling system for improved thermal performance. To be able to determine the Nusselt Number Nu , this flow made numerous assumptions (Nu). The convective of heat transfer coefficient was then calculated using the Nu. The heat flow around the vane was steady and uniform by the authors. The authors then assumes that the Hylton experimental temperature data and It was subjected to a set temperature boundary condition. For the heat transfer calculations reported, the author then used a constant thermal load(Wang, Li and Zhu, 2014; Wang *et al.*, 2015). Finally, the heat transfer coefficient will vary depending on the cooling channel parameters, such as diameter and Reynolds number. Various features of the coolant had to be predicted to accommodate the varied heat transfer coefficient per cooling channel. Assume, for example, that the inlet flow temperature is uniform, and constant, as specified by (Hylton and York,1985; Nirmalan and Hylton, 1989; Wang, Li and Zhu, 2014; Wang *et al.*, 2015).

The number is defined above, and the Prandtl number is as follows in Eq (16):

$$P_r = \frac{c_p \mu}{k_{fg}} \ . \tag{16}$$

Eq. (15) represents the coolant's specific heat capacity, Cp, fluid viscosity, and thermal conductivity, Kfg, which are all represented by Sutherland's Law, as illustrated above. The heat transfer coefficient was then determined using the Nu, as shown in Equation (17) below:

$$h = \frac{k_{fg} N_u}{Dc} \ , \tag{17}$$

where Kfg is thermal conductivity, and Dc is the cooling channel's hydraulic diameter. The heat transfer coefficient can be lowered to Eq. (15-17) by combining Eqs. (11), (16) and (17) (Wang, Li and Zhu, 2014; Wang *et al.*, 2015):

$$h = 0.02424 \cdot C(\lambda, \dot{m}, \mu) D_C^{-1.8}. \quad (18)$$

In Eq. (19) C represents the coefficient associated with a cooling channel and is assumed to be constant cause of the coolant assumptions mentioned previously:

$$C(\lambda, \dot{m}, \mu) = \lambda \cdot (\frac{\dot{m}}{\mu})^{0.8}. \quad (19)$$

The C.S. calculated the HTC using Newton's law of cooling. The heat transfer coefficient is calculated by Ansys using the following equation (20):

$$h = \frac{(q'' \, conduction \, (a))}{[|a| \, T_S - T_w)]} \, , \quad (20)$$

where TS is the standard temperature, where it was supposed to be the average volume, mean bulk temperature for the fluid of the individual channel, Tw is the boundary temperature, for the wall and $\frac{(q'' \, conduction \, (a))}{[|a|}$ is the vector field's heat flux boundary conduction. The heat flux at the boundary considers the impact of both molecular and turbulent diffusion effects on the fluid's boundaries. This analysis was applied to assist in forecasting the average heat transfer statistics of each cooling channel, and the findings on the average heat transfer coefficient (HTC) of the cooling channel are presented in the results section.

2.4. Boundary Condition

C3x boundary condition taken from C3X cascade test conditions code 4311, run 148 (Hylton and York, no date), Tables 1, 2 present the boundary condition which the authors used for simulation.

Table 1. Initial flow condition for the domain

P_0	T_0	M_i	l	T_u	T_w/T_g	M_e (x=0.09836)
321KPa	802K	0.17	0.016m	6.5%	0.73	0.9

Table 2. Cooling channels input boundary conditions

Channel	Mass flow rate(kg/s)	T_{in}(K)
1	0.022	342
2	0.0221	344
3	0.0218	335
4	0.0218	336
5	0.0225	330
6	0.0225	355
7	0.0216	336
8	0.00744	350
9	0.00477	377
10	0.00256	387

2.5. Base model meshing

Achieving mesh independence is an important step in CFD simulations, particularly when performing a conjugate heat transfer (CHT) analysis. Mesh independence means that the solution obtained from the simulation should be relatively insensitive to the mesh density and should converge to the same solution regardless of the number of mesh elements or the mesh geometry. To attain mesh independence, several meshing parameters were employed, including the prism layer mesh, polyhedral mesh, and generalized cylinder mesh. The prism layer mesh is applied to enhance the accuracy of the flow model solution by generating prismatic cells that are orthogonal close to wall surfaces and boundaries, using the core volume mesh. This approach can help enhance the simulation accuracy near the walls, where the flow

exhibits high viscosity. Polyhedral meshes and generalized cylinder meshes are also effective in generating high-quality meshes that can be employed in CHT analysis. These mesh types provide a balanced solution to the challenges of mesh generation by creating an extruded mesh along portions that resemble generic cylinders. This approach can be useful for simulating intricate geometries or areas with high curvature. Finally, the use of the control volume option in Ansys ICEM allows the authors to coarsen or refine a specific portion of the mesh to more precise values. This can be useful for refining the mesh in regions where the flow or heat transfer are particularly important, or where the solution is expected to be highly sensitive to the mesh density. Mesh generated using ICME Ansys, Using Tetrahedrons method, and maximum growth rate 1.2, selecting curvature normal angle 18^{o}. Mesh created to be 3184243 Element, and 682571 nodes. Inflation used with first layer thickness 0.0021 mm, and maximum layer chosen to be 10 Layers, this is very important for CHT accuracy as shown in figure 4, which presents the blade with the flow domain after meshing. Figure 5 presents Full NASA C3X vane meshing with base model cooling channels meshing. Momentum and other scalar transports are most active in near-wall regions where there are larger gradients in the solution variables ('Fluent 6.2 Documentation File, ANSYS Manual, 2006'). The inner layer for this case made from three zones with corresponding wall Y^+ which is non dimensional distance which the same to local Reynolds number, Y+ can be described as viscous sublayer Y^+ less than 5, Y^+ for buffer layer or blinding region is in between 5 to 30, and for fully turbulent Y^+ between 30 to 60. For this case the assumed viscous sublayer with choosing $Y^+ = 1$.

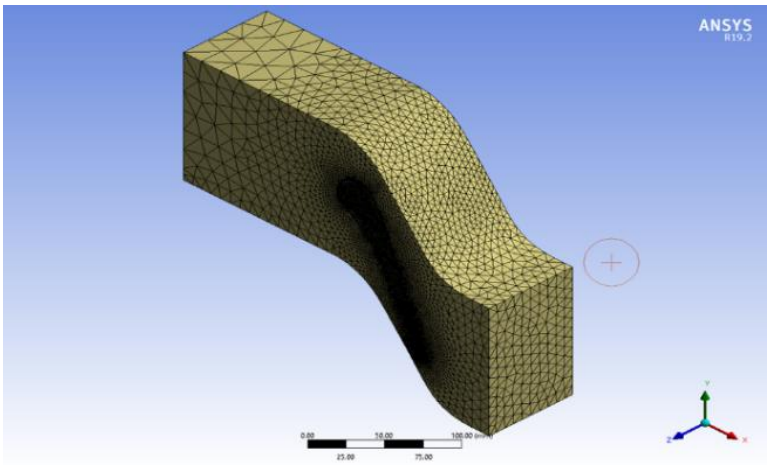
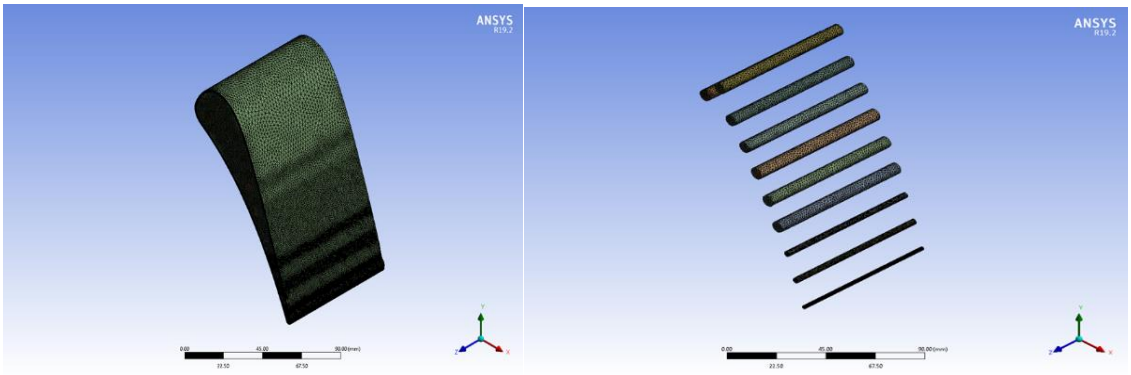


Figure 4. Flow domain meshing configuration



(a) (b)

Figure 5. Full NASA C3X vane meshing: (a) Full NASA C3X vane meshing; (b) Base model cooling channels Meshing

A commonly used threshold for the aspect ratio is around 1.5 to 2.0, meaning that the ratio of the longest edge to the shortest edge should be no greater than 2.0. However, some applications may allow for higher aspect ratios, while others may require much lower aspect ratios, depending on the accuracy and stability requirements. Figure 6 presents the aspect ratio quality metric, and the graph shows that the max elements have average aspect ratio 8.

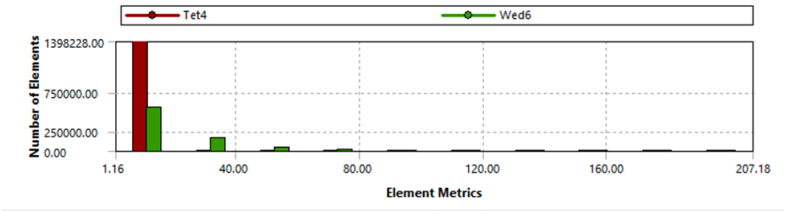
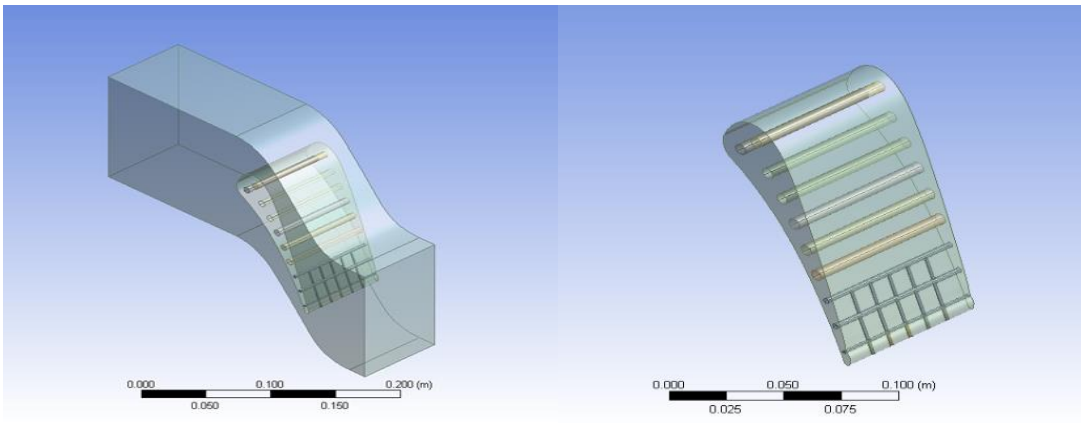


Figure 6. Aspect Ratio mesh Quality

2.6. Optimized model configuration

The optimized jet impingement configuration in the present study. The goal was to achieve an increase in the cooling effectiveness while maintaining similar pressure drops to the base model. The results showed that the optimized jet impingement configuration did indeed lead to an increase in cooling effectiveness by improving the heat transfer coefficient and reducing the temperature of the blade leading edge. This highlights the importance of considering jet impingement parameters in the design of cooling configurations for gas turbine components. Using the same meshing from the base model and applying Glynn research which is confirmed that the heat transfer can be increased with decreasing the jet nozzle diameter, and it's important to determine the jet impingement parameters like the position and diameter of jet nozzle. According to Yamane's experiment that it's important the H/DJ Ratio to be between 2 to 8 where is H is the high between the nozzles and DJ is the jet diameter, with choosing the jet diameter to be 1.94 mm the ratio H/DJ is 8, which is in range ratio according to Yamane Experiment (Yamane *et al.*, 2012), also jet spacing S/DJ ratio to be between 4 to 8, Jet spacing was determine to be 11.44 mm to have jet spacing 5.89. Figure 7 presents the flow domain and optimized turbine blade cooling channels.



(a) (b)

Figure 7. Flow domain and optimized turbine blade cooling channel Model:
(a) Hot Domain configuration; (b) optimized turbine blade cooling channels

Meshing was carried out Using Ansys ICEM the same base model mesh configuration CFD simulation carried out using the same boundary condition which used on base model.

2.7. Validation of the flow domain

Figure 8 presents that domain of absolute pressure flow, the vane's suction side surface experiences the lowest pressure due to its location in the channel throat area where flow velocity is at its highest. In contrast, the stagnation point, situated at the vane's leading edge, encounters the highest pressure. Moving from the leading to the following edge of the pressure side, velocity gradually increases while pressure slowly decreases. However, in the vicinity of the suction surface, velocity initially rises but then declines as it encounters unfavourable pressure gradients from secondary flows. This can lead to boundary layer separation near the suction-side blade surface's trailing edge, a significant cause of profile losses in high-loading blades or vanes. The high loading on the suction side reduces suction side pressure, allowing for an increase in local Mach number and velocity, resulting in supersonic speeds. As the flow approaches supersonic speeds, local shocks form, leading to additional aerodynamic losses such as shock losses or

wave drag. Finally, it's worth noting that the suction surface pressure increases in the region of unfavourable pressure gradients and downstream of the shock in the boundary layer.

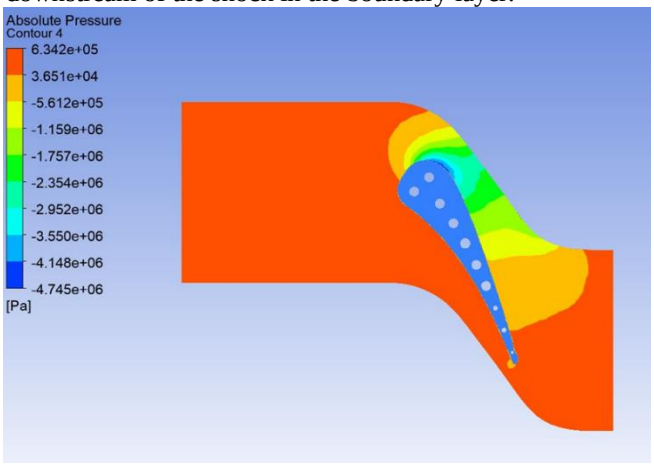


Figure 8. CFD Absolute pressure flow domain

According to the research, the average Mach number at the outlet is 0.765, which is 16.8% lower than the Mach number of 0.88 stated in NASA's reference. The pressure contour plot in the trailing edge area of the outlet region reveals inconsistencies in the exit Mach number computed by the current model compared to Hylton model. Moreover, the pressure distribution on the lower pressure side shows a combination of high and low-pressure areas near the vane's trailing edge, which is a result of boundary layer separation and the impact of secondary flows (Hylton and York, 1985).

3. Results

3.1. Cooling Effect

The current study you are referring to compares the results of different cooling configurations using CFD simulations with Helton's NASA Model and Wang's CFD. The comparison will be presented in three different sections, each focusing on the specific cooling configurations and the important features of each configuration. The study will also present data gathered and assessed in the study, including contour plots of temperature, Pressure, and heat transfer calculations. The comparison will help identify the most effective cooling configuration and provide insight into how to improve the performance of gas turbine blades and vanes.

3.1.1. Configuration of Base model

Figure 9 in the study is referring to Normalized c3x vane span coordinate, which is used for data reduction. Figure 10, Figure 11, and Figure 12 show graphical representations of the mean gauge pressure, mean temperature, and heat transfer coefficient from Hylton's data and the current base model.

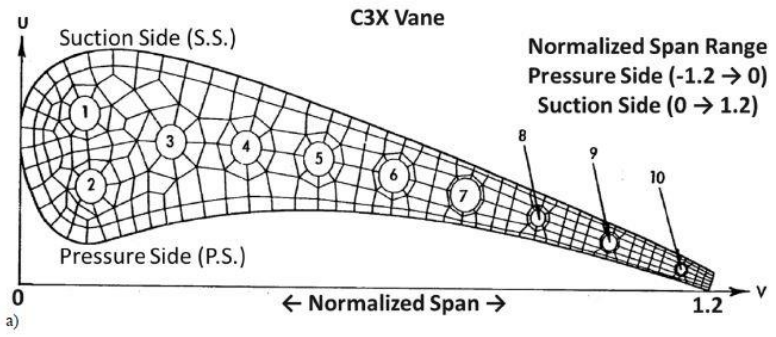


Figure 9. Normalized c3x vane span coordinate which is used for data reduction (Hylton and York, 1985)

This data was generated by matching similar span vs. axial cord positions (xvs.l) to the Hylton data sensor locations, allowing the corresponding mean at that place to be displayed (Hylton and York, 1985). To standardize the data, p/p* were calculated using Hylton's inlet conditions conducted at a nominal gas-stream total temperature of 811 K (Hylton and York, 1985). Figure 10 shows the base model mean gauge pressure data. This comparison allows for an analysis of the current CFD model's accuracy against the NASA model, and the correlation between the two sets of data can be used to validate the current study's CFD results. It is worth noting that, the Hylton's NASA data is widely used as a benchmark in the aeronautical industry, and any correlation between the current study's data and the NASA data will give more credibility to the current study's results compared with C3X Vane Data.

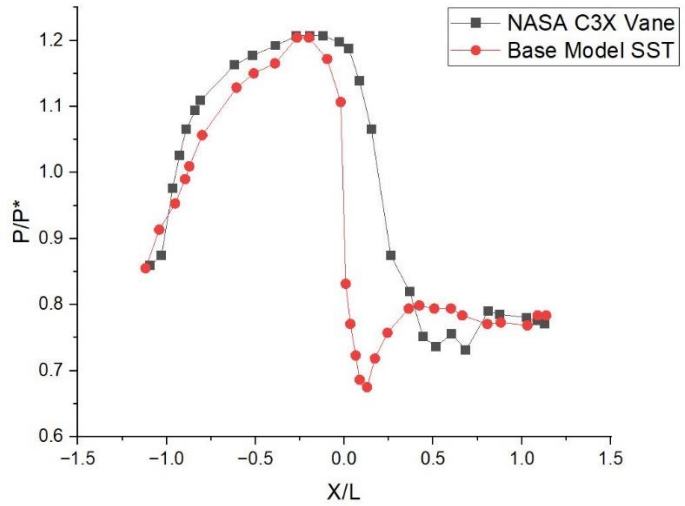


Figure 10. Base model Mean Gauge pressure data compared with C3X vane Data

In the current study, Figure 11 displays a comparison of temperature distribution between the study's data and Helton's NASA C3X model Experiment data, which is normalized between t/811 to mid-span.

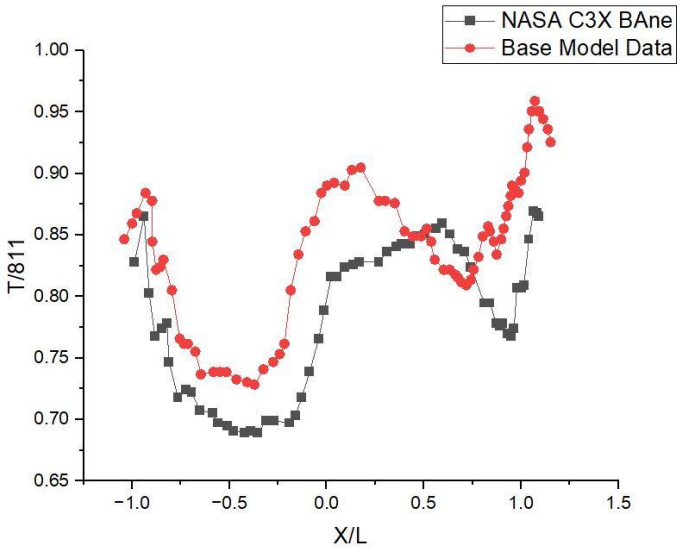


Figure 11. Base Model temperature comparison with NASA C3X Experimental data

Meanwhile, Figure 12 exhibits the local heat transfer coefficient distribution over the turbine blade mid-span. Analysing the temperature distribution comparison allows for an evaluation of the correlation between the two data sets and the accuracy of the current CFD model.

The vane's pressure side follows the Hylton trend, but the current study predicts an overestimated heat transfer coefficient around the vane head and the majority of the suction side. The two models have a 23.36% difference in average h, which may be due to the various assumptions and simplifications in the

current CFD model and potential experimental errors in the NASA data. However, the difference falls within an acceptable range, and the study's results are trustworthy and precise.

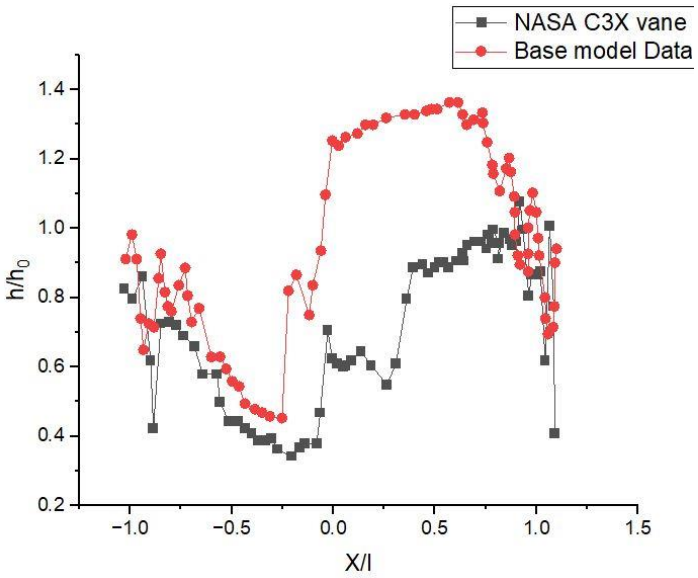


Figure 12. Average heat Transfer coefficient Comparison

In the current study, Figure 13 illustrates the temperature distribution in (k) from the top of the basic blade model configuration. Both models show a similar temperature profile with slight variations. However, the current model indicates a higher temperature profile, especially towards the edge areas, which is most notable on the blade's suction side. These differences are due to the limitations of CFD simulations, as discussed earlier. The temperature in the center of the blade is higher, ranging from 10 to 35K. Nevertheless, the temperature contours in both investigations have the same general pattern, with the vane trailing edge exhibiting the highest temperature of 670+K. By comparing the current study's CFD results and the NASA model results, Wang, and Rossman we can assess the correlation between the two datasets and the accuracy of the current CFD model (Rossman, 2016). The slight variations between the two data sets may be attributed to the various assumptions and simplifications in the current study's CFD model, as well as potential experimental errors in the NASA data (Hylton and York, 1985; Nirmalan and Hylton, 1989; Wang, Li and Zhu, 2014; Wang *et al.*, 2015)

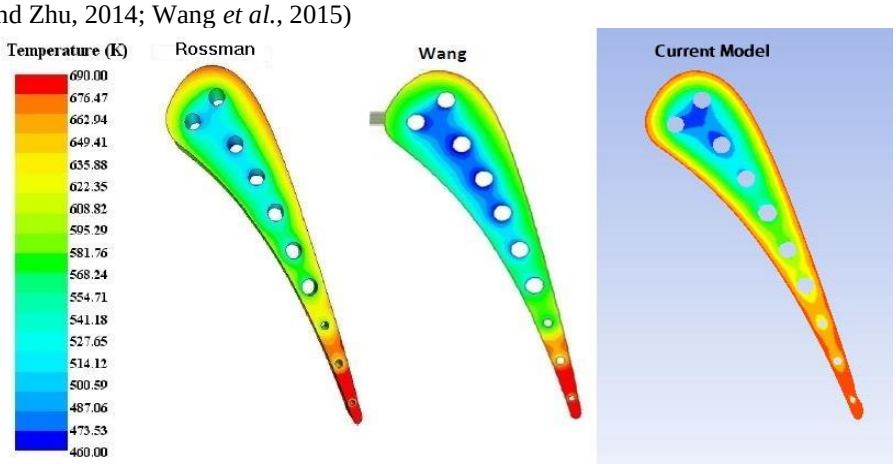


Figure 13. Base model Mean temperature data comparison

3.1.2. Trailing Edge Focus

In this part of the study, recent data is utilized to emphasize the importance and necessity of a jet impingement setup for improved cooling of the trailing edge of turbine vanes. This is significantly cooler compared to the basic case, which ranges from 633K to 685K as shown in figure 14. The comparison

demonstrates the benefits of utilizing a jet impingement cooling configuration, which is more effective in dissipating heat in the trailing edge of the vane where temperatures are highest. This information is essential in designing and optimizing cooling systems for turbine blades and vanes, as it indicates that a triple impingement cooling configuration can greatly enhance the performance and efficiency of gas turbine engines.

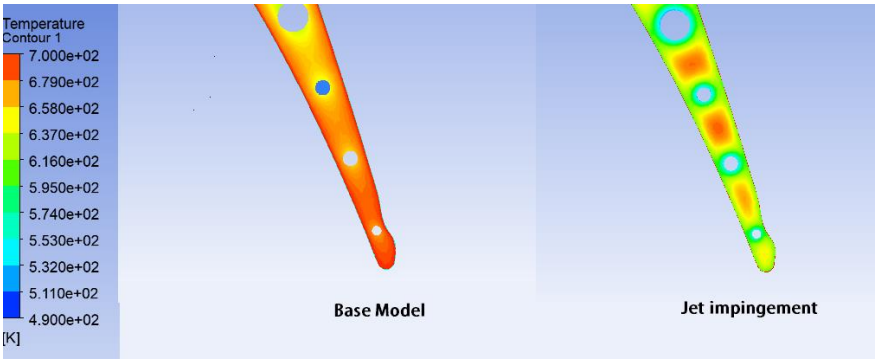


Figure 14. Trailing Edge Temperature comparison between NASA Base Model and optimized model

The network impingement arrangement in the current study exhibits a range that is even cooler than the Base model, with a range from 545K to 598K or 3.1% to 3.9% cooler and a vane that is 14.7% to 20% cooler than the original NASA C3X vane. The trailing edge's tip exhibits the largest temperature drop, as shown above. the base model the vane's very tip has a temperature of 700K, while its trailing edge tip has a temperature of 652.75K. This is a substantially lower temperature than the Baseline and network Cooling jet Impingement, resulting in a 18.3% cooler temperature. Figure 15 views of the temperature contours created in the current study baseline for the three combinations. This highlights the effectiveness of the jet impingement cooling configuration in dissipating heat from the trailing edge of the vane, which is the hottest area of the blade. This information can be used to improve the design and optimization of cooling systems for turbine vanes and blades, resulting in increased performance and efficiency of gas turbine engines.

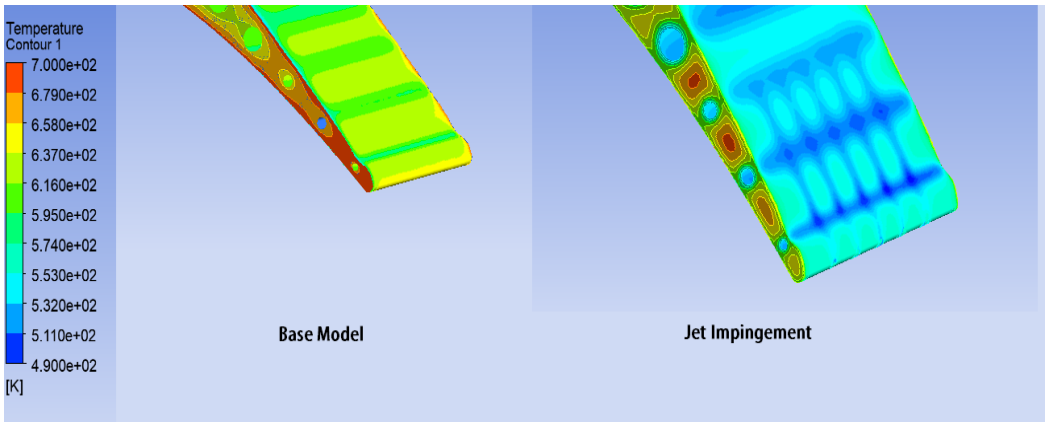


Figure 15. Trailing Edge Temperature comparison between NASA Base Model and optimized model

The Jet impingement setup is an effective method for reducing the temperature at the trailing edge tip of a turbine vane, which is known to be a high-stress area that is susceptible to failure due to high temperatures. The 32.20% decrease in temperature at the trailing edge tip compared to the baseline configuration, and 18.95% decrease compared to the NASA model configuration, represents a substantial improvement in the thermal performance of the turbine and can significantly extend the lifespan of the turbine components.

Figure 16 shows that the triple jet impingement configuration was the most effective in reducing the temperature across the vane when compared to the other two configurations studied in the study. The temperature distribution of this configuration is significantly cooler compared to the other two configurations, which demonstrates that it is the best cooling method among the three investigated. This can help to prevent degradation, corrosion, and vane failure, which are known to occur at high temperatures.

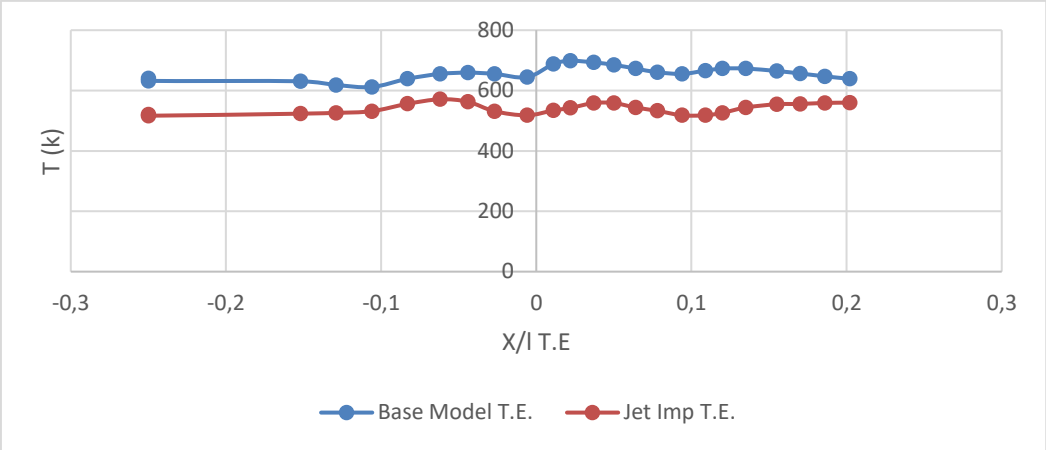


Figure 16. Trailing Edge Temperature comparison between NASA Base Model and optimized model

3.1.3. Conjugate heat transfer

This section of the text is describing a comparison that will be made between calculated and measured average heat transfer coefficients for each cooling channel. The equations that will be used for the calculations are specified as Eqs (14–20). These equations could be the equations used to calculate the heat transfer coefficient using different methods or models. It is likely that the comparison will be used to evaluate the accuracy and reliability of the calculated results in relation to the experimental measurements and to check the validity of the equations used. It could also be used to identify any discrepancies or inconsistencies between the calculated and measured values, and potentially adjust or improvements to the equations or models used for future calculations.

It appears that Figure 17 is a graph or a chart that compares the average heat transfer coefficients calculated for different studies or cases. The caption provided is explaining the information that is shown in the graph. It is saying that the heat transfer coefficient (HTC) of the current study's CFD baseline case is slightly under-predicted for the first eight cooling channels, but the under-prediction becomes more pronounced as the cooling channels approach the trailing edge of the vane. This is explained by the fact that the HTC varies with the hydraulic diameter of the cooling channel, which is consistent with the understanding of heat transfer and fluid dynamics.

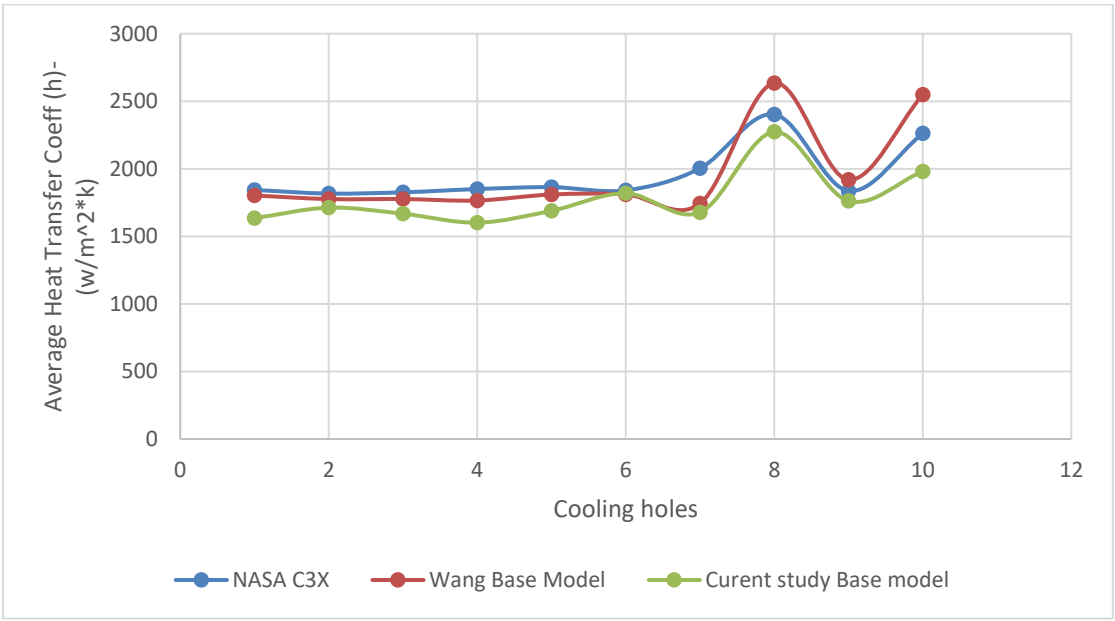


Figure 17. Trailing Edge Temperature comparison between NASA Base Model, Wang model, and optimized model.

This passage presents further details about the cooling channels and their differences in the studies being compared. It notes that the hydraulic diameter of the cooling channels decreases significantly (by up to 59.70%-69.55%) as they approach the vane's trailing edge, which can have a significant impact on the cooling system's performance and heat transfer coefficients. The passage also highlights the variations between the studies, ranging from 2.9-15% between Hylton's original C3X computed data and the current study's CFD baseline case. Moreover, the current study's CFD baseline case differs from Wang's computed data by a range of 2.4-26% in the calculated cooling channel heat transfer coefficients. These findings suggest that the cooling channels near the vane's trailing edge play a more significant role in the heat transfer coefficient, and the results of the current study's CFD model are distinct from previous studies.

This study is explaining the major differences between the current study and previous studies, one of which is that the fully developed flow assumption is not used in the current study. This means that the study is not assuming that the flow inside the cooling channels has reached a steady state and that the velocity and temperature profiles are constant throughout the channel. Instead, the study is considering the variations in the Reynolds numbers of the individual cooling channels, which can affect the heat transfer coefficients.

The current study is comparing the performance of two different cooling configurations, the Base Model configuration and the Jet Impingement configuration, by calculating the average heat transfer coefficient (HTC) for each cooling channel using a specific method or equation. The results of this calculation are then presented in Figure 18. This figure shows the differences in average HTC between the two configurations for each cooling channel.

This comparison can provide insights on how the Jet Impingement configuration affects the cooling performance of the channels and how it compares to the Base Model configuration. It can be used to identify which cooling channels have higher or lower HTC in the Jet Impingement configuration compared to the Base Model configuration, and it can help to understand how the Jet Impingement configuration affects the cooling performance of the channels. Figure 16 shows that there is no significant difference in the average heat transfer coefficient (HTC) of the cooling holes between the Base Model and the Jet Impingement configuration. The small difference between the two cases is relatively small and ranges from 0% to 5%. It was anticipated that the cooling channels 8/9/10, which are in the jet impingement section, would have the greatest difference.

This could be due to a variety of factors such as the geometry of the cooling holes, the Reynolds number of the flow, or the heat transfer model used. The results of this comparison can provide insights on how the Jet Impingement configuration affects the cooling performance of the channels, and it can help to identify which cooling channels have the most significant differences in heat transfer coefficient between the two configurations.

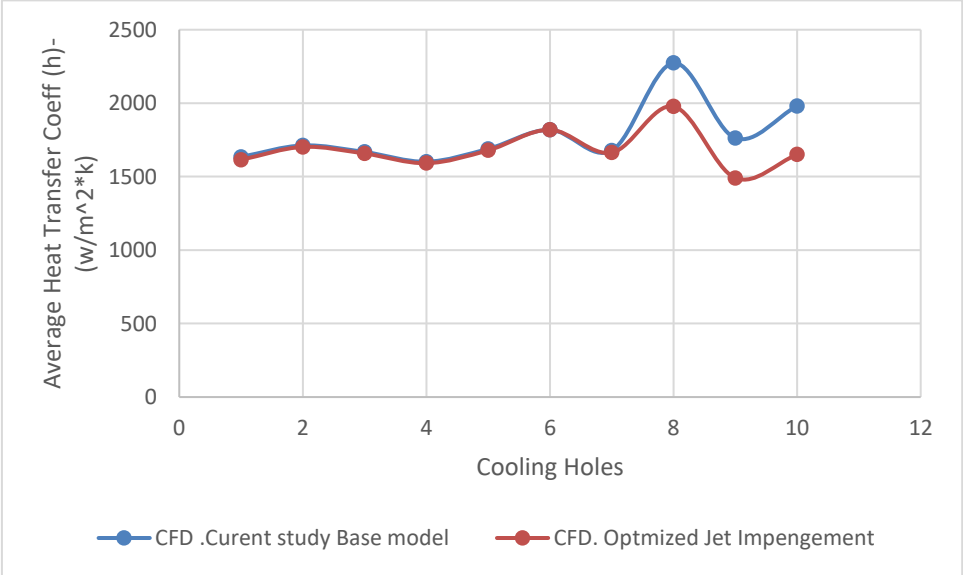


Figure 18. Temperature comparison between NASA Base Model, and optimized model

Figure 19 illustrates a comparison between NASA Base Model and optimized model for the Blade wall heat flux.

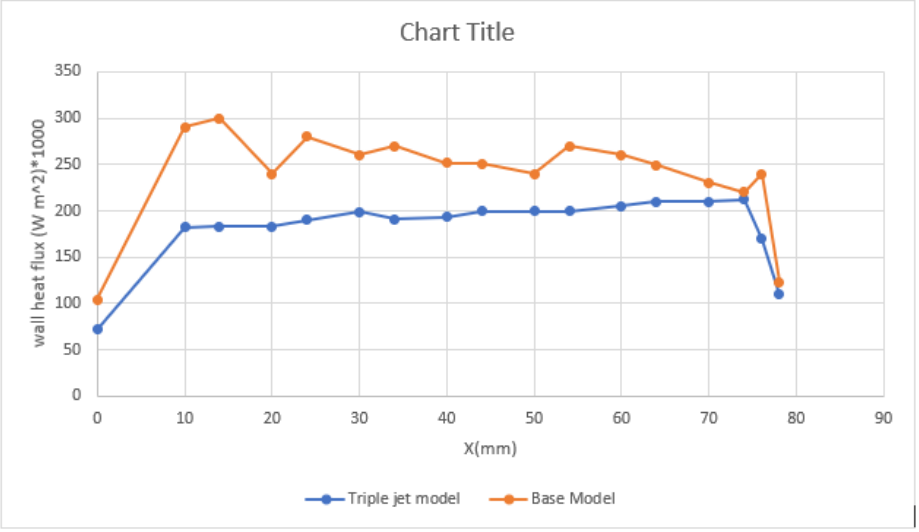


Figure 19. Blade wall heat flux comparison between NASA Base Model, and optimized model

3.1.4. Determination of Cooling effectiveness for the optimized model

Cunha mathematical formula used to calculate the cooling effectiveness (φ) of a forced convection heat transfer system, such as a turbine blade cooling channel (Uysal *et al.*, 2006). The equation considers the temperature difference between the coolant and the wall, the Reynolds number, and the Prandtl number. The general form of the Cunha equation is

$$\varphi = \frac{T_{gas} - T_{metal}}{T_{gas} - T_{c,in}}, \tag{21}$$

where T_{gas} is the temperature of the gas in the fluid domain, T_{metal} is the temperature of the solid which is the blade in our study, and TC, in is the temperature of the coolant which in our case is cold air.

By calculating the cooling effectiveness of a turbine blade with and without a triple impingement system, it is possible to compare the two systems and determine whether the optimized jet impingement system improves the cooling performance of the blade while minimizing losses to the overall turbine system. The cooling effectiveness values can be used as a metric to determine the improvement in cooling and can be used to optimize the design of the cooling system for maximum performance. By comparing the cooling effectiveness values of the two systems, engineers can determine the best design for the turbine blade cooling system and ensure that the blade operates within acceptable temperature limits, which is critical for the longevity and reliability of the turbine. the average coolant temperature as the inlet temperature for the cooling channels, and to model the metal temperature as the temperature of the solid blade and the gas temperature as the temperature of the hot fluid. These are commonly used inputs for calculating the cooling effectiveness. After calculation the cooling effectiveness for the base model and optimized jet impingement model we found it 0.4892 for whole blade and we compare it with the cooling effectiveness for the optimized jet impingement model, which is 0.6936. The results of the comparison between the base model and the optimized jet impingement model suggest that the optimized model has a significantly higher cooling effectiveness. The increase in cooling effectiveness of 29.46% for the whole blade and 28.823% for the trailing edge indicates that the optimized jet impingement design provides improved cooling performance. These results highlight the importance of considering optimized cooling designs for turbine blades to maintain efficient and safe operation.

4. Discussion

The increase in cooling effectiveness of 29.46% for the whole blade and 28.823% for the trailing edge indicates that the optimized jet impingement design provides improved cooling performance. These results highlight the importance of considering optimized cooling designs for turbine blades to maintain efficient and safe operation.

5. Conclusions

The current study revealed a greater temperature profile, particularly towards the edge areas, which is especially noticeable on the blade suction side. These disparities result from the limiting computations of CFD simulations, as mentioned earlier in the discussion. The temperature at the center of the blade appears to be higher, ranging between 10 and 35K. The temperature contours in both investigations, however, exhibit the same overall character, with the vane trailing edge representing the warmest temperature of 670+K. This comparison between the current study's CFD results and the NASA model results allows for an analysis of the correlation between the two sets of data and the accuracy of the current CFD model. The minor differences between the two sets of data can be attributed to the various assumptions and simplifications made in the current study's CFD model, as well as possible experimental errors in the NASA data.

In this specific study, ANSYS FLUENT code was used as a CFD solver, and ANSYS ICEM-CFD was used for mesh generation. ANSYS FLUENT is a widely used commercial CFD software that can solve a wide range of fluid flow and heat transfer problems. ANSYS ICEM-CFD is a tool that can generate high-quality meshes that are suitable for use in CFD simulations. Together, these tools can be used to perform detailed and accurate CFD simulations of the cooling configurations in a gas turbine blade.

The trailing edge of the vane presented previously in Figure 15 is emphasized in this section using a third of the standardized span data. when only looking at the back third of the vane, ranges from 540K to 617K, beginning from the last three segments and sub-holes. This is much cooler than the basic case, which ranges from 633K to 685K. This comparison highlights the advantages of using a jet impingement cooling configuration, which is more effective in dissipating heat at the trailing edge of the blade, where temperatures are highest.

This study is providing additional information about the cooling channels and how they differ in the studies being compared. It states that the cooling channels hydraulic diameter decreases by a significant percentage (up to 49.70%-69.55%) as they affect the vane's trailing edge. This can have a significant impact on the heat transfer coefficients and the performance of the cooling system.

The study also states that there is a difference between the studies, ranging from 2.9-15% between Hylton model, the original C3X calculated data, and the current study's CFD baseline case. Additionally, the current study's CFD baseline case differs from Wang's computed data by a range of 2.4-26% from the cooling channel heat transfer coefficients calculation.

The pressure side of the blade is observed to follow the Hylton model, while the current study predicts a large over-anticipated heat transfer coefficient around the blade head and on the bulk of the suction side. In terms of average heat transfer coefficient, the two models differ by 23.36%.

Optimized jet impingement model we found it 0.4892 for whole blade and we compare it with the cooling effectiveness for the optimized jet impingement model, which is 0.6936, The results of the comparison between the base model and the optimized jet impingement model suggest that the optimized model has a significantly higher cooling effectiveness. The increase in cooling effectiveness of 29.46% for the whole blade and 28.823% for the trailing edge indicates that the optimized jet impingement design provides improved cooling performance. These results highlight the importance of considering optimized cooling designs for turbine blades to maintain efficient and safe operation.

References

1. Ackert, S. (2011) Engine Maintenance Concepts for Financiers Elements of Turbofan Shop Maintenance Costs. 43 pages. PDF available at: http://www.aircraftmonitor.com/uploads/1/5/9/9/15993320/engine_mx_concepts_for_financiers___v2.pdf
2. Brown, G.O. (2002) The History of the Darcy-Weisbach Equation for Pipe Flow Resistance, in Environmental and Water Resources History. Reston, VA: *American Society of Civil Engineers*, pp. 34–43. https://doi.org/10.1061/40650(2003)4.
3. Coletti, F., Scialanga, M. and Arts, T. (2012) Experimental Investigation of Conjugate Heat Transfer in a Rib-Roughened Trailing Edge Channel with Crossing Jets, *Journal of Turbomachinery*, 134(4). https://doi.org/10.1115/1.4003727.
4. Elmenshawy, A.A.A.E. and Alomar, I. (2022) Statistics and Investigation of CF6 Jet Engines Hot Section Failures, pp. 88–98.https://doi.org/10.1007/978-3-030-96196-1_9.
5. Fluent 6.2 Documentation File, ANSYS Manual. (2006).
6. Hylton, L.D. and York, R.E. (1985) *Analytical and Experimental Evaluation of the Heat Transfer Distribution Over the Surfaces of Turbine Vanes*.

7. Nikora, V. (2006) Hydrodynamics of aquatic ecosystems. *Acta Geophysica*, 55(1), 3–10. DOI:10.2478/s11600-006-0043-6
8. Nirmalan, V. and Hylton, L.D. (1989) An Experimental Study of Turbine Vane Heat Transfer with Leading Edge and Downstream Film Cooling. *Heat Transfer; Electric Power; Industrial and Cogeneration. American Society of Mechanical Engineers*, 4. https://doi.org/10.1115/89-GT-69.
9. Nozhnitsky, Y.A. (2018) The Problem of Ensuring Reliability of Gas Turbine Engines, IOP Conference Series: *Materials Science and Engineering*, 302, p. 012082. https://doi.org/10.1088/1757-899X/302/1/012082.
10. Organ, A.J. (2007) Counter-flow spiral heat exchanger – Spirex, *The Air Engine. Elsevier*, 29–38. https://doi.org/10.1533/9781845693602.1.29.
11. Rossman, C.D. (2016) Analysis of a Coupled Micro-and Triple-Impingement Cooling Analysis of a Coupled Micro-and Triple-Impingement Cooling Configuration in the C3X Vane Configuration in the C3X Vane. *Available* at: https://commons.erau.edu/edt.
12. Uysal, U. *et al*. (2006) Heat Transfer on Internal Surfaces of a Duct Subjected to Impingement of a Jet Array with Varying Jet Hole-Size and Spacing, *Journal of Turbomachinery*, 128(1), 158–165. https://doi.org/10.1115/1.2101859.
13. Wang, J., Sundén, B., Zeng, M., and Wang, Q. (2015) Film cooling effects on the tip flow characteristics of a gas turbine blade, *Propulsion and Power Research*, 4(1), 9-22, https://doi.org/10.1016/j.jppr.2015.02.003.
14. Wang, K., Li, H. and Zhu, J. (2014) Experimental study of heat transfer characteristic on jet impingement cooling with film extraction flow, Applied Thermal Engineering, 70(1), 620–629. https://doi.org/10.1016/j.applthermaleng.2014.05.077.
15. Yamane, Y. et al. (2012) Effect of Injection Parameters on Jet Array Impingement Heat Transfer, *International Journal of Gas Turbine, Propulsion and Power Systems*, 4(1), 27–34. https://doi.org/10.38036/jgpp.4.1_27.
16. Zaretsky, E. V., Litt, J. S., Hendricks, R C., Soditus, S M. (2013) *Determination of Turbine Blade Life from Engine Field Data*. Available at: https://ntrs.nasa.gov/search.jsp?R=20120007098.